

Influence of γ Irradiation on the Properties of Polyacrylonitrile Films

S. M. Pawde, Kalim Deshmukh

Department of Physics, University Institute of Chemical Technology, University of Mumbai, Matunga, Mumbai 400019, India

Received 27 January 2008; accepted 21 April 2008

DOI 10.1002/app.28761

Published online 22 August 2008 in Wiley InterScience (www.interscience.wiley.com).

ABSTRACT: In this study, we examined the effects of γ irradiation on the mechanical, thermal, structural, and electrical properties of polyacrylonitrile (PAN). Irradiation doses of 20, 40, 60, 80, and 100 kGy were used, with non-irradiated PAN films serving as control samples. Microhardness measurements, mechanical tests, Fourier transform infrared (FTIR) spectroscopy, differential scanning calorimetry analysis, color determination, X-ray diffraction, and electrical properties were investigated to evaluate the effects of the irradiation treatments on the PAN films. A fair consistency was observed between the microhardness results. Irradiation caused a significant deterioration in the mechanical properties of the samples. The tensile strength and percentage elongation at break decreased with increasing irradiation dose. Similarly, Young's modulus and toughness also decreased with increasing irradiation dose.

The melting and crystallization temperatures decreased, whereas the degree of yellowness increased with increasing irradiation dose. The percentage crystallinity of the PAN film increased with increasing irradiation dose. The FTIR spectra showed that there was a tendency toward a greater effect of γ irradiation on the structure of PAN at higher irradiation doses. The values of the electrical parameters, such as capacitance in parallel, dielectric constant, dielectric loss, resistance in series, resistance in parallel, reactance, and quality factor, increased, whereas the values of capacitance in series, impedance, conductance, susceptance, admittance, and phase angle decreased because of the γ irradiation. © 2008 Wiley Periodicals, Inc. *J Appl Polym Sci* 110: 2569–2578, 2008

Key words: dielectric properties; differential scanning calorimetry (DSC); FTIR; irradiation

INTRODUCTION

Studies on the interaction of high-energy radiation with polymers have attracted the attention of many researchers. This is because high-energy radiation can induce both chain scission and/or crosslinking.^{1,2} For some applications, radiation degradation can be controlled and devoted to achieve a specific property. Radiation processing has been demonstrated on a commercial scale to be a very effective means of improving the end-use properties of polymer materials. Properties such as mechanical and thermal stability, chemical resistance, melt flow processability, and surface properties can be significantly improved by radiation processing.³ γ irradiation is used because of its higher penetrating capability and negligible heat production.^{4,5}

The major chemical changes occurring in polymers as a result of radiation are (a) scission and/or crosslinking of the polymeric chains, with their net effect

determining the changes in the polymer properties; (b) the formation of gases and low-molecular-weight radiolysis products; and (c) the formation of unsaturated bonds.^{6,7} The extent of radiation-induced changes in polymeric materials depends on the polymer type and morphology, the specific additives used to compound the polymers, the type of radiation (i.e., β or γ), the irradiation dose and dose rate (kGy/h) in which irradiation takes place (i.e., absence or presence of oxygen), and the temperature.⁸ Methods for accessing the extent of radiation-induced changes in polymeric materials include mechanical testing⁹ (e.g., tensile strength, percentage elongation at break, compression testing, tear strength, puncture resistance) and physicochemical testing¹⁰ (e.g., thermal testing, sealability, change in crystallinity), colorimetry¹¹ (to measure the degree of discoloration), Fourier transform infrared (FTIR) spectroscopy¹² (to measure structural changes), gas chromatography¹³–mass spectroscopy¹⁴ and/or liquid chromatography–mass spectroscopy¹⁵ (to identify radiolysis products), electron spin resonance spectroscopy¹⁶ (to measure free radicals formation), and rheological testing¹⁷ (i.e., to measure changes in molecular weight).

Polyacrylonitrile (PAN) is a versatile polymer that is widely used for making membranes that offer good resistance to a wide range of solvents.¹⁸ It

Correspondence to: S. M. Pawde (sunita_pawde@yahoo.com).

Contract grant sponsor: All India Council for Technical Education (for funds to procure the Precision LCR meter of Hewlett Packard made by Agilent Technologies).

shows good mechanical strength as a film and is thermally stable. However, it also has some disadvantages, such as a strong hydrophobicity, electrostatic accumulation, and so on because of the lack of segmental mobility resulting from the intensive molecular orientation of the highly polar nitrile groups.¹⁹ It exhibits an unusually high melting temperature (T_m) of 320°C compared with that of other aliphatic polymers.^{20–23} The interactions between polar nitrile groups are responsible for its high T_m . At higher temperatures, the thermal energy of the segment mobility will be higher, which might produce a greater effect in opposing the dipolar interaction forces of the nitrile groups.²⁴

In recent years, interest in the study of the electrical properties of polymers has grown significantly. Some of these have been on fundamental aspects, which are of interest not only for understanding the inherent properties of the material but also for determining many of its practical applications. The dielectric properties, such as the dielectric constant (ϵ) and dielectric loss ($\tan^{-1} A$), of fiber-forming PAN is interesting because of its polar nitrile groups. In addition, γ irradiation has become one of the most common processes used to produce modifications in its physical, chemical, and morphological structures. The thermal expansion coefficient of PAN increases rapidly in the vicinity of 90°C with increasing temperatures.^{25–27} Its high strength; high softening temperature; resistance to weathering, chemicals, water, and cleaning solvents; and soft-wool like feel have made PAN popular for many uses, such as in blankets and various types of clothing.²⁸

Hence, in this investigation, we attempted to study the effect of γ irradiation on the structural, mechanical, and thermal properties of PAN films. Test methods used in this study included mechanical property testing (tensile strength, percentage elongation at break, toughness, and Young's modulus), thermal analysis [T_m and crystallization temperature (T_c)] colorimetry (measurement of degree of discoloration), X-ray diffraction (XRD), and FTIR spectroscopy (identification of structural changes in the polymer as a result of irradiation). The microhardness values of the PAN films were also measured at different irradiation doses. The dielectric properties of pure and γ -irradiated PAN films were measured at an irradiation dose of 25 kGy.

EXPERIMENTAL

Materials

The PAN used in this study was obtained in powder form from the Naval Material Research Laboratory (Ambernath, India). Dimethyl formamide was obtained from Merck, Ltd. (Mumbai, India).

Film preparation

To prepare the PAN films, the polymer was dissolved in dimethyl formamide solution at 60°C, and the solution was poured into a glass pellet. Upon drying, the solution stood at room temperature for 2 h, and a thin transparent film of PAN was obtained. The prepared films were stored in vacuum desiccators for further study.

γ irradiation

The γ irradiation of the square-shaped ($0.01 \times 0.01 \text{ m}^2$), 40–50 μm thick specimens were carried out with a high-energy source Co^{60} Gamma Chamber-900 (irradiation source) supplied by BARC (Mumbai, India). Samples were irradiated with various doses ranging from 20 to 100 kGy (20, 40, 60, 80, and 100 kGy). The films were exposed to γ irradiation in air at a dose rate of 0.40 M rad/h.

Characterization

The irradiated samples were indented at room temperature by a mhp-160 microhardness tester with a Vickers's diamond pyramidal indenter (JENA, Japan) with a square base and a 136° pyramidal angle attached to a Carl Zeiss NU₂ universal research microscope (JENA, Japan). The Vickers hardness number (H_v) was calculated from the following relation:

$$H_v = 1.854 \times L/d^2 (\text{kg/mm}^2)$$

where L is the load (kg) and d is the diagonal of indentation (mm). For each test, the duration was 30 s. For each load, at least five indentations were made at different points of the specimen, and the average H_v was calculated. During the test, the specimens were kept strictly horizontal and rigid.

Visual color was measured by a Hunter colorimeter model DP-900 optical sensor (Hunter Lab Associates, Road Reston, VA) in terms of lightness (L) from black (0) to white (100), a from green (–) to red (+), and b from blue (–) to yellow (+). The instrument (45°/0° geometry, 10° observer) was calibrated with a standard white tile ($L = 91.58$, $a = -0.79$, $b = -0.35$). A glass Petri dish containing the PAN film was placed beneath the light source to record the L , a , and b values.

The mechanical properties of the pure and irradiated PAN films were tested on a Lloyd LR10K universal tensile machine. A thin film sample 4 cm long and 1 cm wide (ASTM D 638) was gripped between the two jaws of the tensile machine. The crosshead speed was kept at 5 mm/min. The average value was calculated from a set of a minimum of 10 measurements.

The FTIR spectroscopy of the pure and irradiated PAN films was performed with an attenuated total

reflection FTIR spectrophotometer (Paragon 500 model, PerkinElmer, Beaconsfield, Buckinghamshire, UK) in the wave-number range 400–4000 cm^{-1} with a resolution of 4 cm^{-1} . The FTIR spectra were taken in a transmittance mode.

The thermal analysis was performed with a PerkinElmer DSC-7 differential scanning calorimeter at a heating rate of 10°C/min under a nitrogen atmosphere. The melting studies were performed in the temperature range 50–350°C.

XRD studies of the pure and irradiated PAN films were recorded with a Bruker D8 Advance XRD meter (Rigaku Corp., Tokyo, Japan) with Ni-filtered Cu K α radiation with a wavelength (λ) of 1.54060 Å with a graphite monochromator. The scan was taken in a 2θ range of 5–40° with a scanning speed and step size of 1°/mm and 0.01°, respectively. The percentage crystallinity was measured by a formula given elsewhere.²⁹

The dielectric properties were measured at normal temperature and pressure conditions with 4284A, Precision Inductance, Capacitance and Resistance meter (Agilent Technologies Ltd., Santa Clara, CA) within the frequency range 20 Hz to 1 MHz and various direct-current (dc) bias potentials from 0 to 40 V. The samples were tested only as a function of frequency. The diameter of the film was around 40 mm. The films were silver coated from both sides for better electrode contact.³⁰ The specialty of this impedance (Z) analyzer was inbuilt dc bias potential variation facilities, which enabled us to apply simultaneous dc potentials along with an alternating-current signal to measure the overall electrical parameters. The fixture assembly attached to this instrument was designed to take observations at normal temperature and pressure conditions only. The electrical properties were measured at an irradiation dose of 25 kGy only.

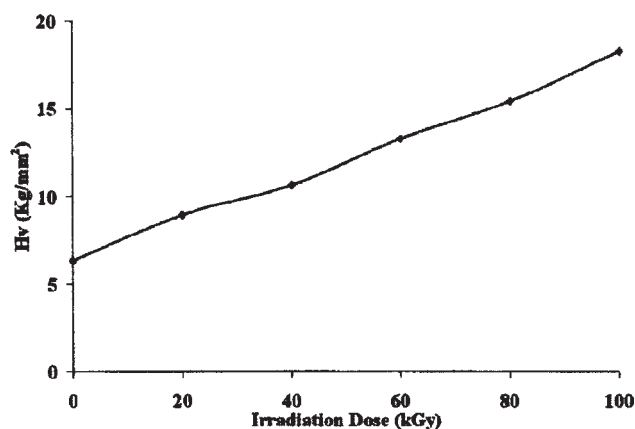


Figure 1 Variation of H_v with different irradiation doses for PAN at a load of 60 g.

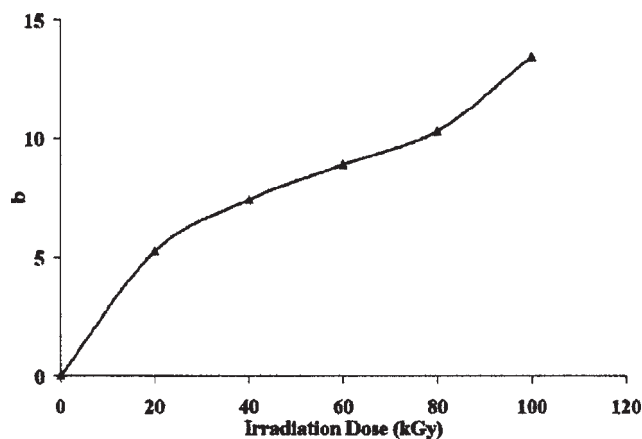


Figure 2 Hunter b values of PAN versus irradiation dose.

RESULTS AND DISCUSSION

Microhardness measurements

The microhardness has been found to be a nondestructive means of characterizing the mechanical performance of polymers.³¹ This technique can also be used to study radiational crosslinking in polymeric materials. Figure 1 shows the effect of various doses of γ irradiation, ranging from 20 to 100 kGy, on microhardness of the surface of pure PAN at a load of 60 g.

It is clear from the figure that the microhardness increased with increasing radiation dose up to 100 kGy for PAN. The increase in microhardness for the irradiated samples compared with the nonirradiated (0 kGy) sample confirmed radiation-induced oxidative degradation in PAN. The oxidative degradation began at 20 kGy and stabilized with further increases in the dose up to 100 kGy. Increases in the dose further increased the radiation-induced oxidative degradation between the PAN chains up to a dose of 100 kGy. Thus, there was a clear indication of the predominance of oxidative degradation in pure PAN as a result of γ irradiation. The higher level of microhardness in the PAN may have been due to the greater extent of intermolecular interaction between the functional groups of pure PAN chains.

Color measurements

The results obtained from color analysis before and after γ irradiation are shown in Figures 2–4. The data in Figure 2 show significant differences in the Hunter b values between the nonirradiated and irradiated samples. An increase in irradiation dose increased the Hunter b color values. As a result, the irradiated samples became more yellow in relation to the nonirradiated samples. The Hunter L values (Fig. 3) decreased with increasing irradiation dose.

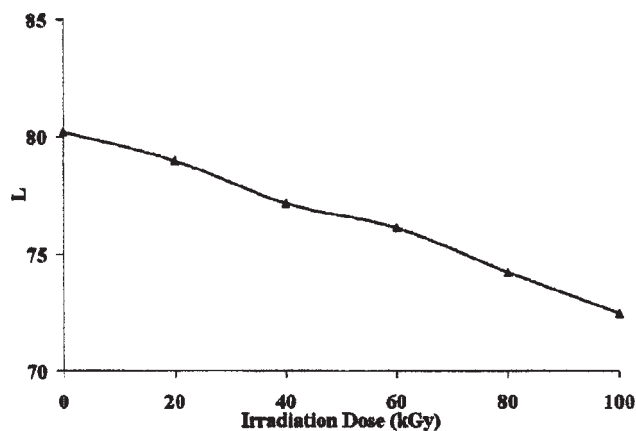


Figure 3 Hunter *L* values of PAN versus irradiation dose.

Thus, the nonirradiated samples had a brighter appearance than the irradiated samples. Irradiation also caused a decrease in the Hunter *a* values (Fig. 4). Further statistical analysis of the total color difference (ΔE) values, an indicator of the total color difference between the nonirradiated and irradiated samples, showed that there was a significant increase in this parameter with increasing irradiation dose (Fig. 5).

ΔE of the samples was calculated according to the following equation:

$$\Delta E = [(\Delta L)^2 + (\Delta a)^2 + (\Delta b)^2]^{1/2}$$

The symbol Δ expresses the differences between the standards (control sample) and the irradiated samples' color values. The degree of discoloration (yellowing) was directly related to the type of stabilizing additives used during the compounding of the polymeric material. On the basis of the previous data, we postulated that the ΔE values for PAN may be used as a basis for developing a method to monitor the intensity of γ irradiation.⁹

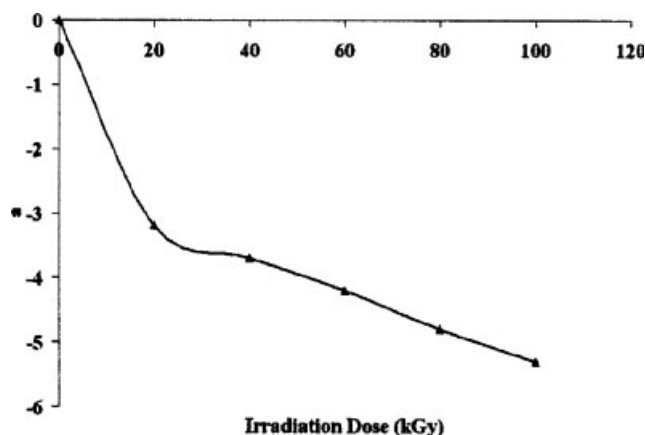


Figure 4 Hunter *a* values of PAN versus irradiation dose.

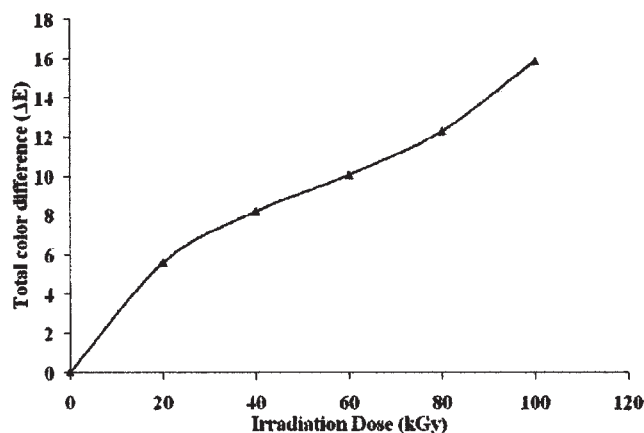


Figure 5 ΔE values of PAN versus irradiation dose.

Mechanical properties

The results of the mechanical tests of the PAN films irradiated at different irradiation doses are summarized in Table I. Figure 6 presents the results of the tensile strength. The tensile strength of the PAN films decreased with increasing irradiation dose. This shows that there was a tendency toward a greater effect of γ irradiation on the tensile strength of the PAN films. Figure 7 is the plot of the percentage elongation at break against the irradiation dose. The elongation at break decreased with increasing irradiation dose. Similarly, the Young's modulus and toughness of the PAN films also decreased with increasing irradiation dose, which is shown in Figures 8 and 9, respectively. Thus, the decrease in mechanical properties at higher doses was attributed to the radiation-induced oxidative degradation of polymers in the presence of air.^{14,32} The extent of the radiation-induced oxidative degradation depends on the nature of polymer, the radiation dose and dose rate, and the crystallinity of the polymer.³²⁻³⁵ The lower the polymer crystallinity is, the easier it is for oxygen to penetrate into the crystalline region of the polymer, and consequently, the higher the oxidation potential will be.³⁶ When we compared our results with those of Fintzou et al.,⁴ we observed that γ

TABLE I
Mechanical Properties of the PAN Films Irradiated at Different Doses

Irradiation dose (kGy)	Elongation (%)	Tensile strength (MPa)	Young's modulus (MPa)	Toughness (MPa)
0	17.58	44.81	1296.3	2.97
20	15.93	42.19	1210.2	2.90
40	14.28	39.85	1095.7	2.84
60	13.12	37.55	1015.6	2.76
80	11.64	34.22	966.2	2.70
100	10.61	31.72	885.7	2.63

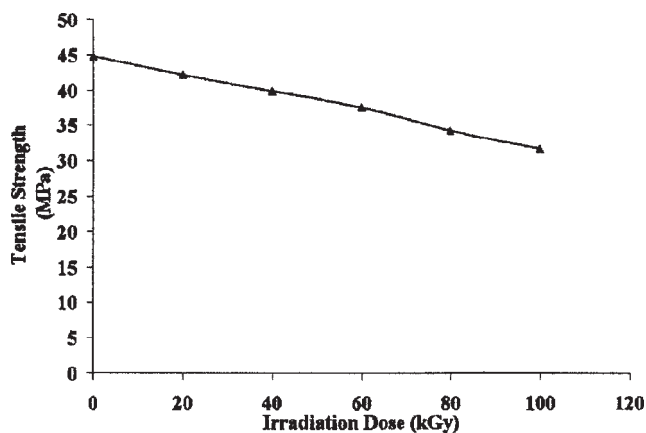


Figure 6 Variation of the tensile strength with different irradiation doses.

irradiation *in vacuo* caused less degradation in the mechanical properties of the polymers than γ irradiation in air.

Infrared spectroscopy

Additional information on the changes in the chemical structure of the PAN films induced by γ irradiation was obtained by FTIR spectroscopy. Infrared spectra of the original and irradiated PAN films are shown in Figure 10. From these spectra, we observed that irradiation at various doses affected the molecular structure of the PAN films. The characteristic stretching band of the nitrile group of PAN appeared at 2240 cm^{-1} . The bands at 3460 and 3390 cm^{-1} were assigned to the asymmetric and symmetric stretching modes of NH_2 groups, respectively. Typical characteristics of the absorption band for PAN at 2250 cm^{-1} corresponding to $\text{C}\equiv\text{N}$ were clearly visible.^{37,38} The band at 2810 cm^{-1} corresponded to CH stretching vibrations. Also, peaks near $2900\text{--}3000\text{ cm}^{-1}$ were assigned to CH stretching vibrations. After irradiation at doses of 20-, 40-, and

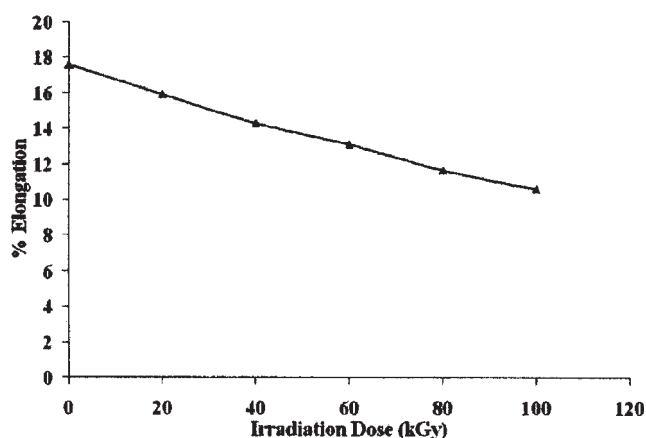


Figure 7 Variation of the percentage elongation with different irradiation doses.

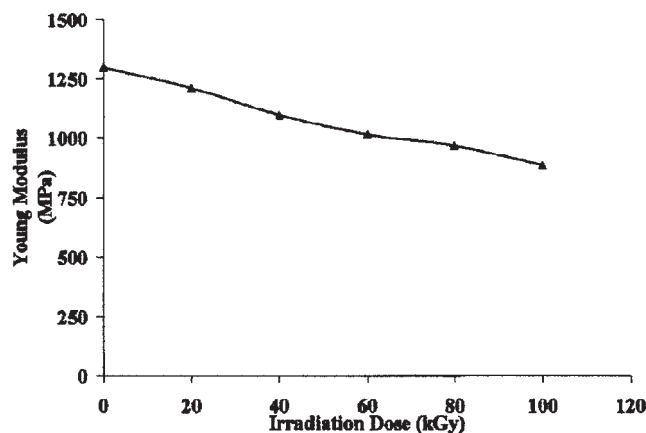


Figure 8 Variation of the Young's modulus with different irradiation doses.

60-kGy changes were observed in the region $400\text{--}1200$ and $3000\text{--}4000\text{ cm}^{-1}$. The intensity of the peaks in these regions increased with increasing irradiation dose up to 60 kGy. At higher irradiation doses (80 and 100 kGy), a single broad peak was observed in the region $3000\text{--}4000\text{ cm}^{-1}$. This study showed that there was a tendency toward greater effect of γ irradiation on the structure of PAN at higher irradiation doses.

Thermal analysis

The shape of the calorimetric melting curve provides valuable information on the thermal history and structural characteristics of a sample.³⁹ The melting and crystallization behaviors for the nonirradiated and irradiated PAN films are given in Figures 11 and 12, respectively. The results obtained from the differential scanning calorimetry curves are summarized in Table II. The recorded differential scanning calorimetry curves obtained for the control and irradiated PAN films showed only one melting peak. This provided evidence that the polymer studied

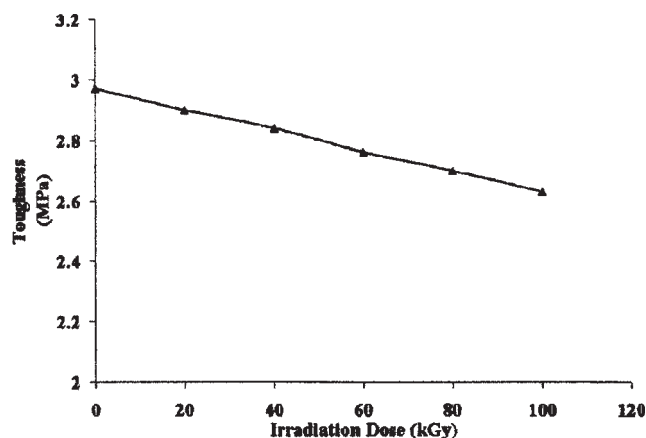


Figure 9 Variation of the toughness with different irradiation doses.

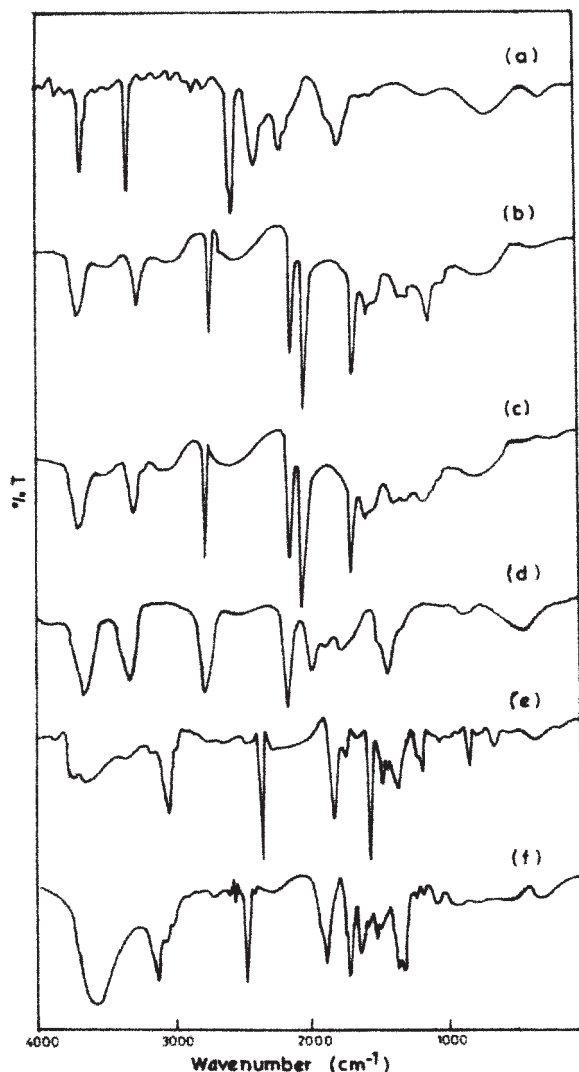


Figure 10 FTIR spectroscopy of PAN irradiated at different doses: (a) 0, (b) 20, (c) 40, (d) 60, (e) 80, and (f) 100 kGy.

was characterized by one crystalline form.^{13,40} T_m and the specific melting enthalpy (ΔH) decreased with increasing irradiation dose. It was, therefore, clear that the polymer became more amorphous during irradiation. Irradiation caused a decrease in the length of the macromolecular chains, crosslinking, and other modifications in the crystalline structure. This degradation mechanism was accentuated by the presence of air, which simultaneously led to oxidation. Similarly, irradiation caused a decrease in T_c from 285.6 to 265.5°C and increased the heat of crystallization (ΔH_c) from 497.9 to 563.6 J/g. This suggested that γ irradiation accelerated crystallization through heterogeneous nucleation and increased the degree of crystallinity. In addition, the width of the crystalline peaks of all of the samples broadened. Thus, the restricted segmental motion near the organic-inorganic interfaces accounted for the broadening in T_c . Obviously, in the presence of air, all

deterioration phenomena in the polymer matrix were pronounced.

ΔH is directly related to the percentage crystallinity variation ($\Delta\tau$) as calculated by following equation:

$$\Delta\tau = (\Delta H - \Delta H^*)/\Delta H \times 100$$

where ΔH^* is the melting enthalpy of the irradiated sample and ΔH is the melting enthalpy of the control sample. As shown in Table II, ΔH^* decreased with increasing irradiation dose, which led to an increase in the degree of crystallinity.

XRD

The observed XRD patterns of the pure and γ irradiated PAN films are shown in Figure 13. We

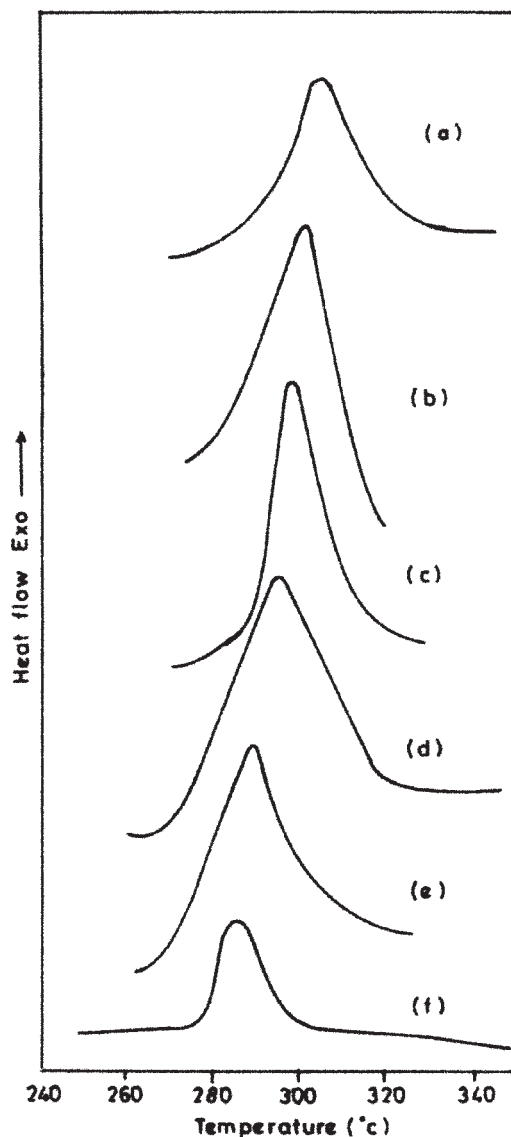


Figure 11 Melting thermograms of PAN irradiated at different doses: (a) 0, (b) 20, (c) 40, (d) 60, (e) 80, and (f) 100 kGy.

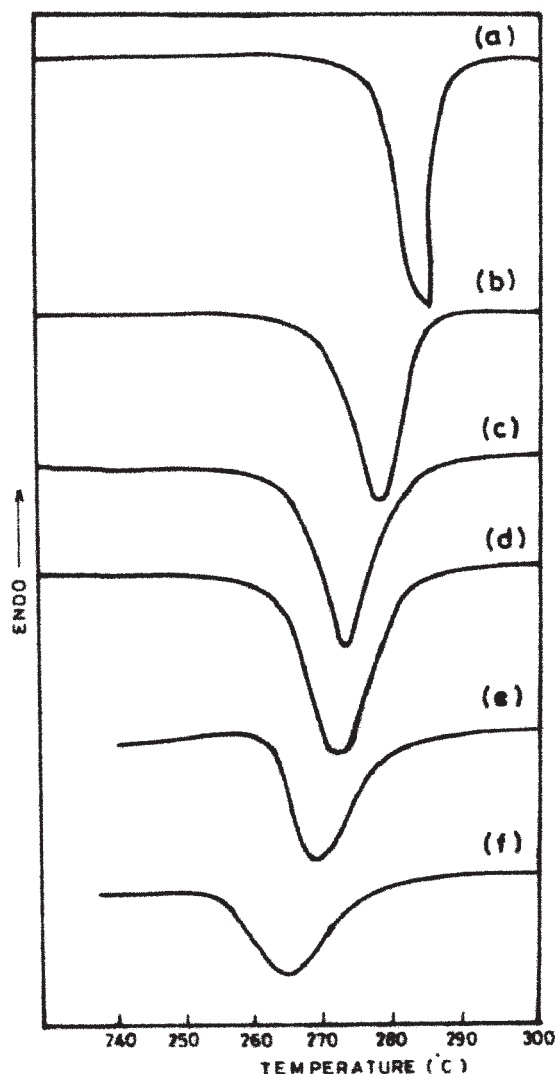


Figure 12 Crystallization thermograms of PAN irradiated at different doses: (a) 0, (b) 20, (c) 40, (d) 60, (e) 80, and (f) 100 kGy.

observed a relatively sharp peak at $2\theta = 17.3^\circ$ ($d = 5.121 \text{ \AA}$) and a broad noncrystalline peak at $2\theta = 28.2^\circ$ ($d = 3.161 \text{ \AA}$) for the PAN film. PAN is unusual in that even atactic molecules can crystallize. The presence of a sharp reflection superimposed over diffuse scattering in these diffraction patterns is

characteristic of the crystalline and amorphous phases of conventional semicrystalline polymers.^{41,42} This diffractogram, when compared with the curves reported by Imai et al.⁴³ for various types of PAN structures (completely amorphous and with hexagonal and orthorhombic crystalline forms), showed a resemblance to the curve for the hexagonal crystalline form in the two-phase structure of PAN. The characteristic peak at 17.3° corresponded to the orthorhombic PAN reflection.⁴⁴ This XRD study of PAN film thus suggests the presence of two well-defined phases, amorphous and crystalline, in the PAN sample.

Table III shows the 2θ values, d -spacing, and percentage crystallinity obtained by XRD. As shown in Table III, irradiation caused a decrease in the 2θ values and increased the d -spacing values. For an irradiation dose of 20 kGy, two broad peaks were observed at $2\theta = 17.1^\circ$ ($d = 5.181 \text{ \AA}$) and $2\theta = 26.4^\circ$ ($d = 3.373 \text{ \AA}$). Similarly, at an irradiation dose of 40 kGy, two broad peaks were observed at $2\theta = 16.9^\circ$ ($d = 5.242 \text{ \AA}$) and $2\theta = 24.6^\circ$ ($d = 3.615 \text{ \AA}$). The intensity of all of these peaks increased with increasing irradiation dose. At higher irradiation doses of 60, 80, and 100 kGy, single XRD peaks were observed at $2\theta = 16.5^\circ$ ($d = 5.368 \text{ \AA}$), $2\theta = 15.2^\circ$ ($d = 5.824 \text{ \AA}$), and $2\theta = 14.8^\circ$ ($d = 5.980 \text{ \AA}$), respectively. This means that the dipole-dipole or hydrogen bonding interactions with the nitrile groups of the polymer were crystallized. On the basis of the observed XRD scans, it was apparent that the crystallinity of PAN increased with increasing irradiation dose.

Electrical properties

PAN is highly polar; therefore, we thought it would be interesting to investigate the electrical properties of pure and γ -irradiated PAN films with a Precision LCR meter. An attempt was made to correlate the dielectric properties and resistive properties of the pure and γ -irradiated PAN films. The dielectric properties of polymers depend in general on the structure, crystallinity, morphology, and presence of other additives.⁴⁵ The permittivity of polymers is

TABLE II
Crystallization and Melting Behaviors of PAN Irradiated at Different Doses

Irradiation dose (kGy)	T_c ($^\circ\text{C}$)	T_m ($^\circ\text{C}$)	ΔH_c (J/g)	ΔH_{melt} (J/g)	Crystallinity (%)
0	285.6	305.4	497.9	-239.19	51.10
20	278.3	301.6	552.2	-111.51	53.38
40	274.5	298.3	562.1	-105.55	55.87
60	272.4	296.8	589.7	-100.96	57.79
80	268.8	290.4	553.8	-92.76	61.21
100	265.5	284.2	563.6	-88.69	62.92

ΔH_{melt} , specific melting enthalpy.

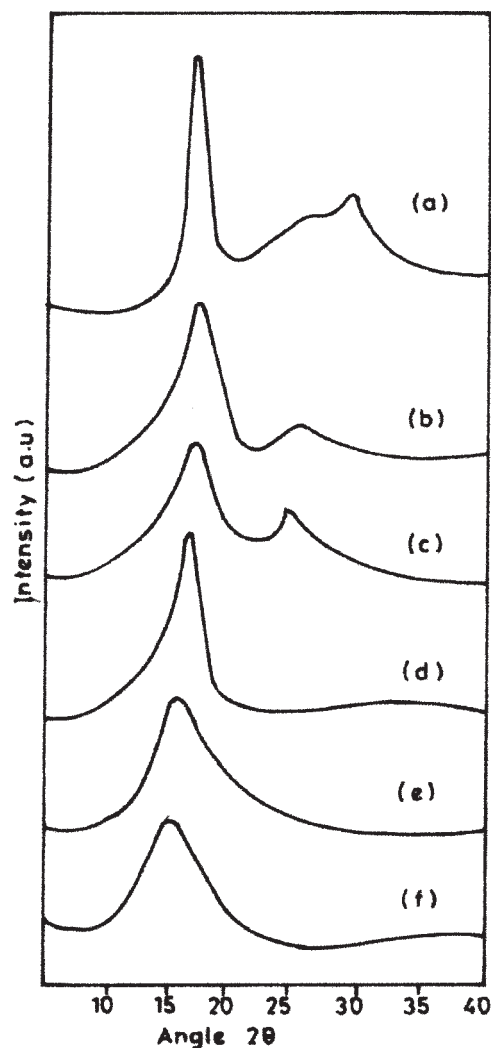


Figure 13 XRD of PAN irradiated at different doses: (a) 0, (b) 20, (c) 40, (d) 60, (e) 80, and (f) 100 kGy.

influenced by interfacial effects (i.e., those due to polarization arising from the differences in the conductivities of two phases).⁴⁶ The ϵ and $\tan^{-1} A$ values as a function of frequency for the pure PAN film within the frequency range 20 Hz–1 MHz for

TABLE III
XRD Results for the PAN Films Irradiated at Different Doses

Irradiation dose (kGy)	2 θ values	$d = n\lambda / (2 \sin \theta)$ (Å)	Crystallinity (%)
0	17.3	5.121	53.21
	28.2	3.161	
20	17.1	5.181	54.36
	26.4	3.373	
40	16.9	5.242	56.62
	24.6	3.615	
60	16.5	5.368	57.27
80	15.2	5.824	59.89
100	14.8	5.980	61.42

n , order of diffraction.

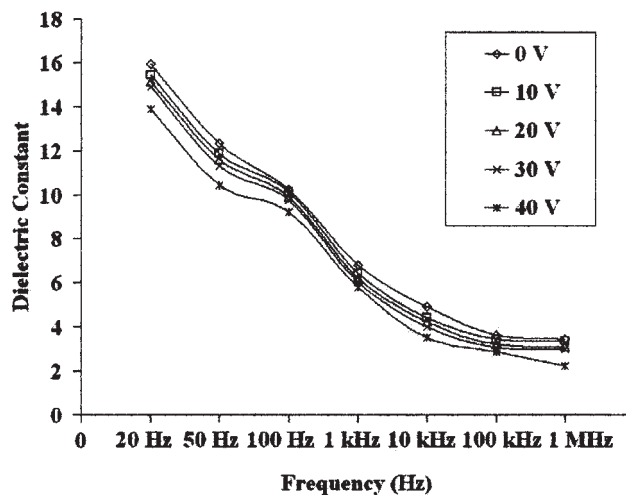


Figure 14 ϵ as a function of the frequency of the pure (0 kGy) PAN film.

various dc bias potentials of 0–40 V are shown in Figures 14 and 15, respectively. ϵ was the highest at a frequency of 20 Hz, and with further increases in frequency and dc bias potential, the trend decreased. Hence, the ϵ values were directly proportional to the dc bias potential applied across the PAN film. $\tan^{-1} A$ was also highest at a lower frequency, and with further increases in frequency and dc bias potential, the trend decreased. The decrease in $\tan^{-1} A$ with frequency may have been caused by dielectric dispersion. Hence, the magnitude of $\tan^{-1} A$ of the PAN films was also directly proportional to the dc bias potential applied across the sample. This may have been due to the polarization of PAN dipoles at lower frequencies.

The ϵ and $\tan^{-1} A$ values as a function of frequency of the PAN film irradiated at 25 kGy are shown in Figures 16 and 17, respectively. As shown in these figures, the values of ϵ and $\tan^{-1} A$ were enhanced because of γ irradiation. The enhancement of the electrical properties after γ irradiation was

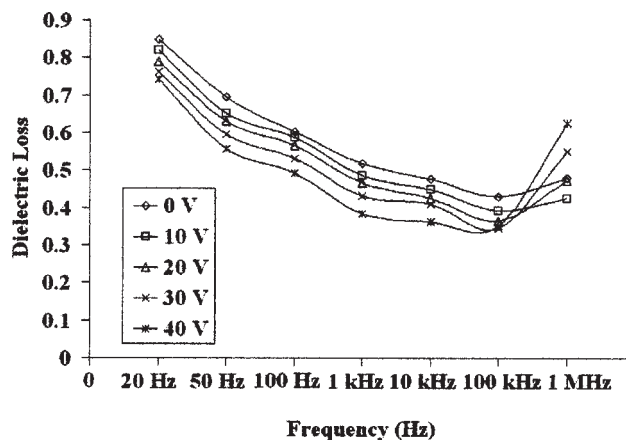


Figure 15 $\tan^{-1} A$ as a function of the frequency of the pure (0 kGy) PAN film.

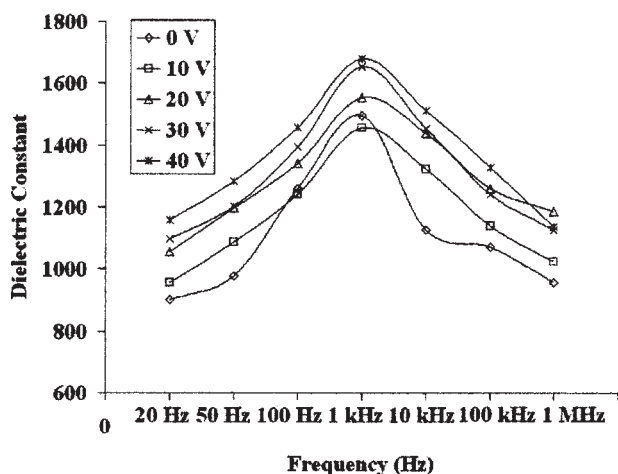


Figure 16 ϵ as a function of the frequency of the PAN film irradiated at 25 kGy.

due to orientation/crosslinking of the PAN molecules with segmental chains of the microporous structure.^{30,47} The irradiated film showed structural and morphological changes compared to the pure PAN film with the shift of the polarization peak from one frequency to another. These morphological and structural changes affected the polarizing frequency of the irradiated PAN films. Therefore, any additional dc bias potential would not show any significant impact on the polarization.

The resistance in series (R_s), resistance in parallel (R_p), capacitance in series (C_s), capacitance in parallel (C_p), Z , conductance (G), reactance (X), susceptance (B), admittance (Y), phase angle (θ), and quality factor (Q) of the pure and γ -irradiated PAN films were measured simultaneously while the dielectric properties were measured, and the values are given in Table IV. As shown in Table IV, the values of C_p , ϵ , $\tan^{-1} A$, R_s , R_p , X , and Q increased, whereas the values of C_s , Z , G , B , Y , and θ decreased after γ irradiation.

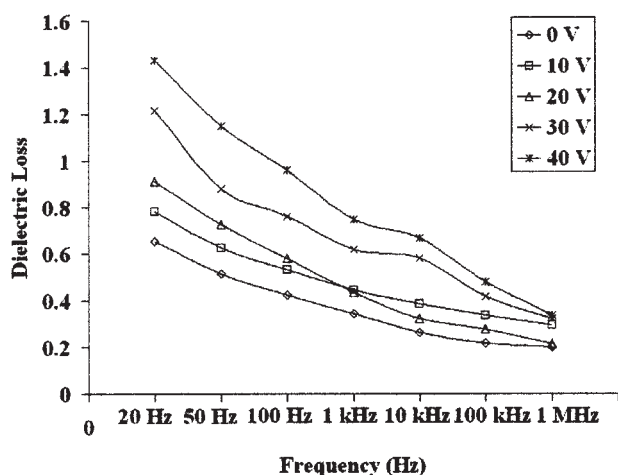


Figure 17 $\tan^{-1} A$ as a function of the frequency of the PAN film irradiated at 25 kGy.

TABLE IV
Electrical Parameters Recorded by the LCR Meter at Various Frequencies and dc Bias Potentials for the PAN Films Irradiated at 25 kGy

Electrical parameter	Pure PAN film	γ -irradiated PAN film
C_p	652 pF, 20 V, 1 kHz	958 pF, 40 V, 100 Hz
C_s	759 nF, 40 V, 1 kHz	660 pF, 40 V, 100 Hz
ϵ	15.936, 0 V, 20 Hz	1678.48, 40 V, 100 Hz
$\tan^{-1} A$	0.849, 0 V, 20 Hz	1.432, 0 V, 20 Hz
R_s	2.54 M Ω , 0 V, 20 Hz	2.9 M Ω , 0 V, 100 Hz
R_p	6.28 M Ω , 0 V, 20 Hz	10.15 M Ω , 0 V, 100 Hz
Z	33.98 M Ω , 0 V, 20 Hz	15.42 M Ω , 0 V, 20 Hz
X	3.075 M Ω , 10 V, 1 MHz	4.51 M Ω , 0 V, 20 Hz
G	893 μ S, 40 V, 1 MHz	235 μ S, 40 V, 1 MHz
B	13.71 mS, 40 V, 100 kHz	2.725 mS, 0 V, 1 MHz
Y	14.4 μ S, 40 V, 100 kHz	2.737 μ S, 0 V, 1 MHz
θ	136°, 10 V, 50 Hz	85.4°, 0 V, 1 MHz
Q	3.46, 30 V, 10 kHz	12.4, 10 V, 1 MHz

tion. The decrease in the electrical properties with increasing irradiation dose may have been due to the delocalization of charge carriers at higher irradiation doses.⁴⁸ Thus, we can say that γ irradiation at higher doses had a greater effect on dielectric properties of the PAN films.

CONCLUSIONS

This study, involving the γ irradiation of PAN films at various irradiation doses of 20, 40, 60, 80, and 100 kGy, showed that the color of the films changed after γ irradiation. The change in color of the PAN films after γ irradiation could be used to develop a sensor for γ -ray dosimetry. The microhardness of the PAN films increased with increasing irradiation dose. γ irradiation caused the deterioration of the color (especially the Hunter b value), mechanical properties (tensile strength, percentage elongation, Young's modulus, and toughness), thermal properties (T_m , ΔH , and T_c), and structural properties of PAN. FTIR spectra showed that there was a tendency toward a greater effect of γ irradiation on the structure of PAN at higher irradiation doses. T_m and ΔH of PAN decreased with increasing irradiation dose. γ irradiation decreased the maximum T_c of PAN and decreased the width of the crystallization peak, which suggested heterogeneous nucleation and a hindered mobility of the polymer chain, resulting in an increase in the degree of crystallinity. The XRD results show that the crystallinity of PAN increased with increasing irradiation dose. γ irradiation had a greater effect on the electrical properties of the PAN films. The values of C_p , ϵ , $\tan^{-1} A$, R_s , R_p , X , and Q increased and the values of C_s , Z , G , B , Y , and θ decreased with γ irradiation. γ irradiation had a greater effect on the aforementioned properties of PAN.

References

1. El-Naggar, A. M.; Kim, H. C.; Lopez, L. C.; Wikes, G. L. *J Appl Polym Sci* 1989, 47, 1655.
2. El-Naggar, A. M.; Lopez, L. C.; Wikes, G. L. *J Appl Polym Sci* 1990, 39, 427.
3. Song, C.; Kerluke, D. R. Presented at the 63rd Annual Technical Conference of the Society of Plastic Engineering (ANTEC), New York, 2003.
4. Fintzou, A. T.; Badeka, A. V.; Kontominas, M. G.; Riganakos, K. A. *Radiat Phys Chem* 2006, 75, 87.
5. Brody, A. L.; Marsh, K. S. *The Wiley Encyclopedia of Packaging Technology*, 2nd ed.; Wiley: New York, 1997; p 696.
6. Buchala, R.; Schutter, C.; Bogl, K. W. *J Food Prot* 1993, 56, 991.
7. Riganakos, K. A.; Koller, W. D.; Ehlermann, D. A. E.; Beuer, B.; Kontominas, M. G. *Radiat Phys Chem* 1999, 54, 527.
8. Goulas, A. E.; Riganakos, K. A.; Kontominas, M. G. *Radiat Phys Chem* 2004, 69, 441.
9. Kabeel, M. A.; Sokar, T. Z. N.; Shahin, M. M. *Radiat Phys Chem* 1991, 38, 199.
10. Sevil, U. A.; Guven, O. *Radiat Phys Chem* 1995, 46, 875.
11. Thorat, H. B.; Prabhu, C. S.; Suresh Kumar, K.; Pandya, M. V. *J Appl Polym Sci* 1997, 59, 1769.
12. Demertzis, P. G.; Franz, R.; Welle, F. *Packag Technol Sci* 1999, 12, 119.
13. Yogoubi, N.; Peron, R.; Legendre, B.; Grossiord, J. L.; Ferrier, D. *Nucl Instrum Methods Phys Res B* 1999, 151, 247.
14. Jahan, M. S.; King, M. C.; Hoggard, W. O.; Sevo, K. L.; Parr, J. E. *Radiat Phys Chem* 2001, 62, 141.
15. Krupa, I.; Luyt, A. S. *Polym Degrad Stab* 2001, 72, 505.
16. Hassanpour, S.; Khoylou, F. *Nucl Instrum Methods B* 2003, 208, 358.
17. Grosu, E.; Papa, M.; Tomescu, A.; Nemes, E.; Zaharescu, T.; Jipa, S.; Setenscu, R.; Vasile, C. *Nucl Instrum Methods B* 2003, 208, 220.
18. Deepak, A. M.; Ashwini, K. *J Appl Polym Sci* 2000, 77, 1782.
19. Chang, W. N.; Young, H. K.; Sohk, W. K. *J Appl Polym Sci* 1999, 74, 2258.
20. Kriegbaum, W. R.; Tokita, N. *J Polym Sci* 1960, 43, 467.
21. Gupta, A. K.; Navin, C. *J Polym Sci Polym Phys Ed* 1980, 18, 1125.
22. Ghyl, M. B.; Whang, K. C. *J Appl Polym Sci* 2002, 84, 2505.
23. Lijima, T.; Tomoi, M.; Tochimoto, T.; Kakikuchi, H. *J Appl Polym Sci* 1991, 43, 463.
24. Gupta, A. K.; Maiti, A. K. *J Appl Polym Sci* 1982, 27, 2409.
25. Hayakawa, R.; Nishi, T.; Arisawa, K.; Wada, Y. *J Polym Sci* 1967, 5, 165.
26. Howard, W. H. *J Appl Polym Sci* 1961, 5, 303.
27. Saito, S.; Nakajima, T. *J Appl Polym Sci* 1959, 2, 93.
28. Bahadur, P.; Sastry, N. V. *Principles of Polymer Science*; Narosa: New Delhi, India, 2003.
29. Manjunath, B. R.; Venkatraman, A.; Stephan, T. *J Appl Polym Sci* 1973, 17, 1091.
30. Gupta, A. K.; Singhal, R. P.; Agarwal, V. K. *Polymer* 1981, 22, 285.
31. Gonzalez, A.; Jesus Martin, G.; Jose Antonio, D. S. *J Appl Polym Sci* 1986, 3, 717.
32. Dole, M. *Radiat Phys Chem* 1991, 37, 65.
33. Wilski, H. *Radiat Phys Chem* 1987, 29, 1.
34. Allen, D. W.; Leathard, D. A.; Smith, C. *Radiat Phys Chem* 1991, 38, 461.
35. Buchala, R.; Boess, C.; Bogl, K. W. *Appl Radiat Isot* 2000, 52, 404.
36. Kashiwabara, H.; Shimada, S.; Hori, Y. *Radiat Phys Chem* 1991, 37, 43.
37. Stupp, S. I.; Carr, S. H. *J Polym Sci Polym Phys Ed* 1977, 15, 485.
38. Coleman, M. M.; Petcavich, R. J. *J Polym Sci Polym Phys Ed* 1978, 16, 821.
39. Perera, R.; Albano, C.; Gonzalez, J.; Silva, P.; Ichaza, M. *Polym Degrad Stab* 2004, 85, 741.
40. Hytiri, S.; Goulas, A. E.; Riganakos, K. A.; Kontominas, M. G. *Radiat Phys Chem* 2006, 75, 416.
41. Gupta, A. K.; Singhal, R. P. *J Polym Sci* 1983, 21, 2243.
42. Cullity, B. D. *Elements of X-Ray Diffraction*; Addison-Wesley: Reading, MA, 1978; p 102.
43. Imai, Y.; Minami, S.; Yoshihara, T.; Joh, Y.; Saito, H. *J Polym Sci Polym Lett Ed* 1970, 8, 281.
44. Sawai, D.; Miyamoto, M.; Kanamoto, T.; Ito, M. *J Polym Sci Part B: Polym Phys* 2000, 38, 2571.
45. Abd-El-Messieh, S. L.; Eid, M. A. M.; Hussein, A. I. *J Appl Polym Sci* 2002, 86, 540.
46. Schifani, R.; Spadro, G.; Cassata, F.; Valenza, A. *Eur Polym J* 1995, 3, 841.
47. Saad, A. L. G.; Aziz, H. A.; Dimitry, O. I. H. *J Appl Polym Sci* 2004, 9, 1540.
48. Anand, J.; Palaniappan, S.; Siddaramiah Srinivasan, P.; Sathyanarayan, D. N. *Eur Polym J* 1999, 35, 499.